Journal of Human Evolution 141 (2020) 102748

Contents lists available at ScienceDirect

Journal of Human Evolution

journal homepage: www.elsevier.com/locate/jhevol

News and Views

New observations of the nasal fossa and interorbital region of *Shoshonius cooperi* based on microcomputerized tomography

E. Christopher Kirk [a, b, *], Ingrid K. Lundeen [a]

[a] Department of Anthropology, University of Texas at Austin, SAC 4.102, 2201 Speedway Stop C3200, Austin, TX, 78712, USA
[b] Jackson School Museum of Earth History, University of Texas at Austin, J. J. Pickle Research Campus, 10100 Burnet Road, PRC 6-VPL, R7600, Austin, TX, 78758, USA

ARTICLE INFO

Article history:
Received 20 August 2019
Accepted 27 January 2020
Available online xxx

Keywords:
Omomyid
Omomyoid
Omomyiform
Haplorhine
Primate
Eocene

1. Introduction

For approximately 75 years after its initial description (Granger, 1910), the early Eocene omomyoid *Shoshonius cooperi* was known only from dentognathic remains (Szalay, 1976; Szalay and Delson, 1979). However, collecting in 1985–1991 by field crews from the Carnegie Museum of Natural History at the Buck Springs Quarries (Lostcabinian; ~50.5 Ma) yielded an abundance of new specimens of *Shoshonius*, including cranial (Beard et al., 1991; Beard and MacPhee, 1994) and postcranial (Dagosto et al., 1999) materials. These new fossils led to a reassessment of the phylogenetic position of *Shoshonius* and revealed that the taxon exhibits a mosaic of primitive and derived features compared with extant haplorhines. In particular, *Shoshonius* has been identified as sharing a suite of derived cranial features with extant tarsiers, including overlap of the auditory bulla by flanges of the basioccipital and alisphenoid, narrowing of the basioccipital and basisphenoid between the left and right auditory bullae, choanae that are narrow and dorsally 'peaked,' orbits that are very large relative to cranial size, and the presence of a 'reduced snout' (Beard et al., 1991; Beard and MacPhee, 1994). These features raised the possibility that Omomyoidea is paraphyletic and that *Shoshonius* is more closely related to extant tarsiers than are other omomyoids (Beard et al., 1991; Beard and MacPhee, 1994). Nevertheless, other researchers have pointed out that tarsiers and anthropoids share a number of derived cranial features not seen in *Shoshonius*, including a postorbital septum that incorporates contact between the alisphenoid and zygomatic, division of the auditory bulla into a tympanic cavity proper and an anterior accessory cavity by a transverse septum, a 'perbullar' pathway for the internal carotid artery, and extreme reduction or loss of the stapedial artery and canal (Cartmill and Kay, 1978; Cartmill, 1980; MacPhee and Cartmill, 1986; Ross, 1994; Kay et al., 2008). Cladistic analyses of these cranial features either recovered *Shoshonius* and other omomyoids as stem tarsiiforms (Beard and MacPhee, 1994) or as stem haplorhines (Ross et al., 1998). The known postcranial anatomy of *Shoshonius* is largely primitive compared with living tarsiers (Dagosto et al., 1999; Boyer et al., 2013) and thus provides little information regarding the question of whether *Shoshonius* is more likely to be a stem tarsiiform or a stem haplorhine. More recent phylogenetic analyses of very large character-taxon matrices including both craniodental and postcranial characters have favored the conclusion that *Shoshonius* and other omomyoids are stem tarsiiforms (Seiffert et al. 2010, 2018; Ni et al., 2013, 2016). If correct, these analyses would imply that some of the derived cranial features shared by extant tarsiers and anthropoids evolved in parallel.

Following the initial descriptions of cranial anatomy in *Shoshonius* (Beard et al., 1991; Beard and MacPhee, 1994), researchers have used a variety of methods to provide additional information about phylogenetically and functionally significant cranial features in the taxon. Comparative analyses of orbit morphology in primates demonstrated that *Shoshonius* has larger orbits than nocturnal strepsirrhines of comparable cranial length (Kay and Kirk, 2000) but is similar to extant strepsirrhines when orbit size is examined relative to molar size (Heesy and Ross, 2001). A comparative analysis of infraorbital foramen area in mammals revealed that *Shoshonius* resembles other omomyoids and extant euarchontans generally in possessing a relatively small infraorbital foramen

* Corresponding author.
E-mail address: eckirk@austin.utexas.edu (E.C. Kirk).

https://doi.org/10.1016/j.jhevol.2020.102748

(Muchlinski and Kirk, 2017). A preliminary report of the internal cranial anatomy of *Shoshonius* based on μCT scans highlighted several derived features shared with tarsiers, including the presence of an apical interorbital septum (AIOS) and a "very crowded posterior nasal cavity, the posterior pole of which lies ventral to the closely approximated orbits" (Rossie and Beard, 2004: 106A). Smith and Rossie (2006: 154) subsequently noted that the AIOS of *Shoshonius* "[takes] the place of the olfactory recess." The first analysis of semicircular canal morphology in *Shoshonius* based on μCT scans revealed that the taxon lacks the very large canal radii of curvature relative to body mass seen in extant tarsiers (Silcox et al., 2009). This aspect of inner ear morphology is probably plesiomorphic and is consistent with the absence of derived postcranial adaptations for vertical clinging and leaping in *Shoshonius* (Dagosto et al., 1999; Boyer et al., 2013). Similarly, μCT-based quantification of cross-sectional areas of canals for the intratympanic branches of the internal carotid artery demonstrated that *Shoshonius* lacks the derived extreme reduction or loss of the stapedial canal seen in extant haplorhines (Boyer et al., 2016). Most recently, Rossie et al. (2018) used μCT scans to quantify the orientation of the nasolacrimal canal (NLC) in both living and fossil primates. This analysis revealed that *Shoshonius* resembles extant haplorhines and differs from the omomyoids *Microchoerus* and *Rooneyia* in possessing a vertically oriented NLC. Although living

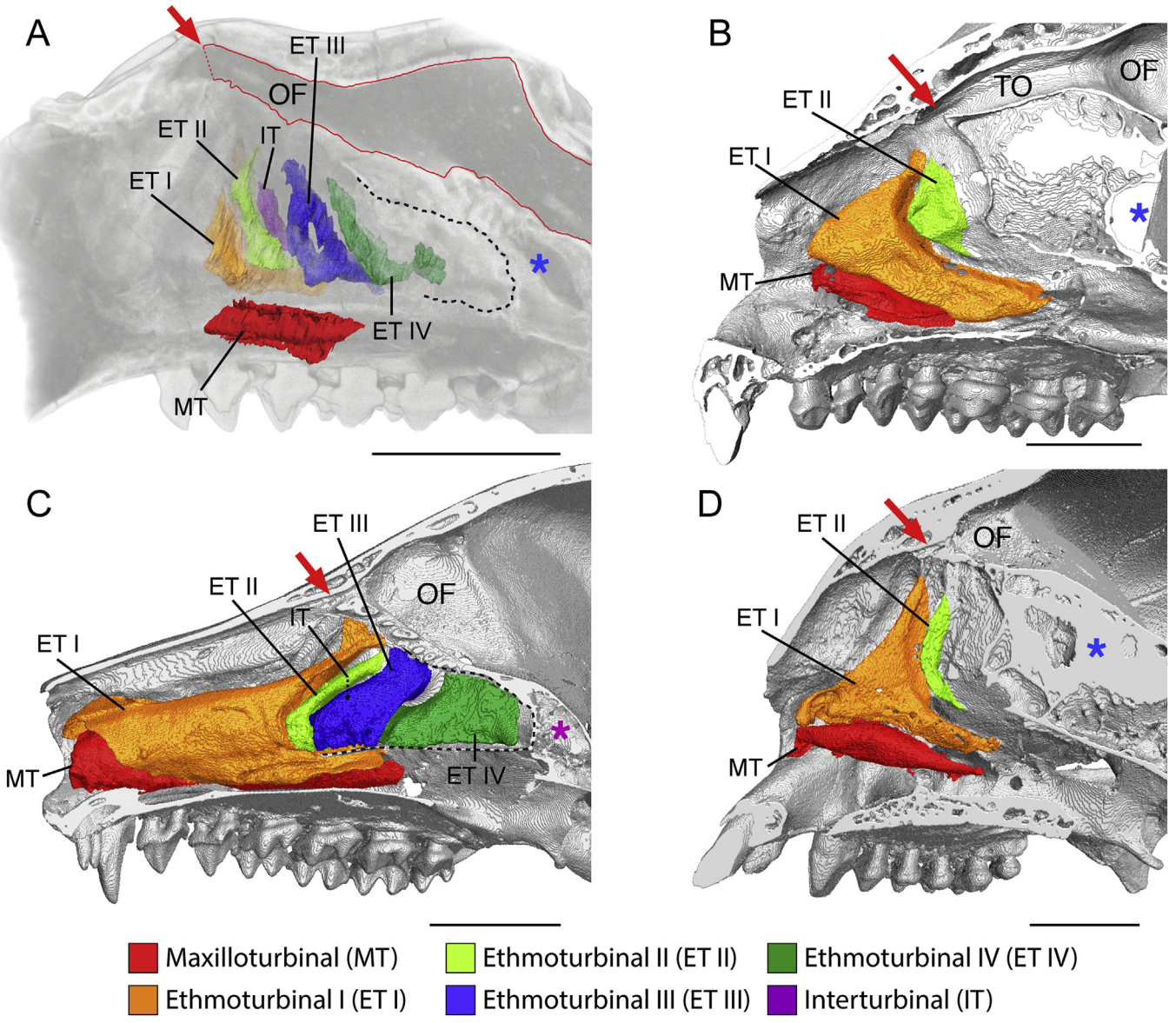

Figure 1. Parasagittal cross sections through the nasal cavities of: A) *Shoshonius cooperi* (CM 31366); B) western tarsier (*Cephalopachus bancanus*, USNM 317189); C) Zanzibar bushbaby (*Galago zanzibaricus*, MCZ 38912); D) saddleback tamarin (*Saguinus fuscicollis*, MCZ 15324). Nasoturbinals and frontoturbinals are not labeled because these structures are either poorly preserved or missing in CM 31366. For extant taxa (B–D), only the right nasal fossa is shown, with the view looking laterally toward the medial surfaces of the turbinals. In *Shoshonius* (A), the ethmoturbinals and interturbinal in the right nasal fossa are figured, with the surrounding matrix and bone rendered translucent to expose the medial faces of these turbinals. However, the maxilloturbinal figured for *Shoshonius* is the better-preserved left maxilloturbinal, which was mirrored into the right nasal fossa to facilitate comparisons with extant taxa. The cut margin of the olfactory recess is shown as a dashed black line in A and C. The cut margin of the endocranial cavity is shown as a solid red line in A. The boundaries of the olfactory recess and endocranial cavity in CM 31366 were traced manually in Adobe Illustrator based on our observations of slice-by-slice renderings of the scan in Avizo. Abbreviations and symbols: OF = olfactory fossa (distorted by crushing in *Shoshonius*); TO = tubus olfactorius; red arrow = anterior margin of the cribriform plate (approximate in *Shoshonius*); blue asterisk in A, B, D = location of the apical interorbital septum; purple asterisk in C = narrowest part of the interorbital region (bilaminar with an intervening space). Scale bars = 5 mm. (For interpretation of the references to color in this figure legend, the reader is referred to the Web version of this article.)

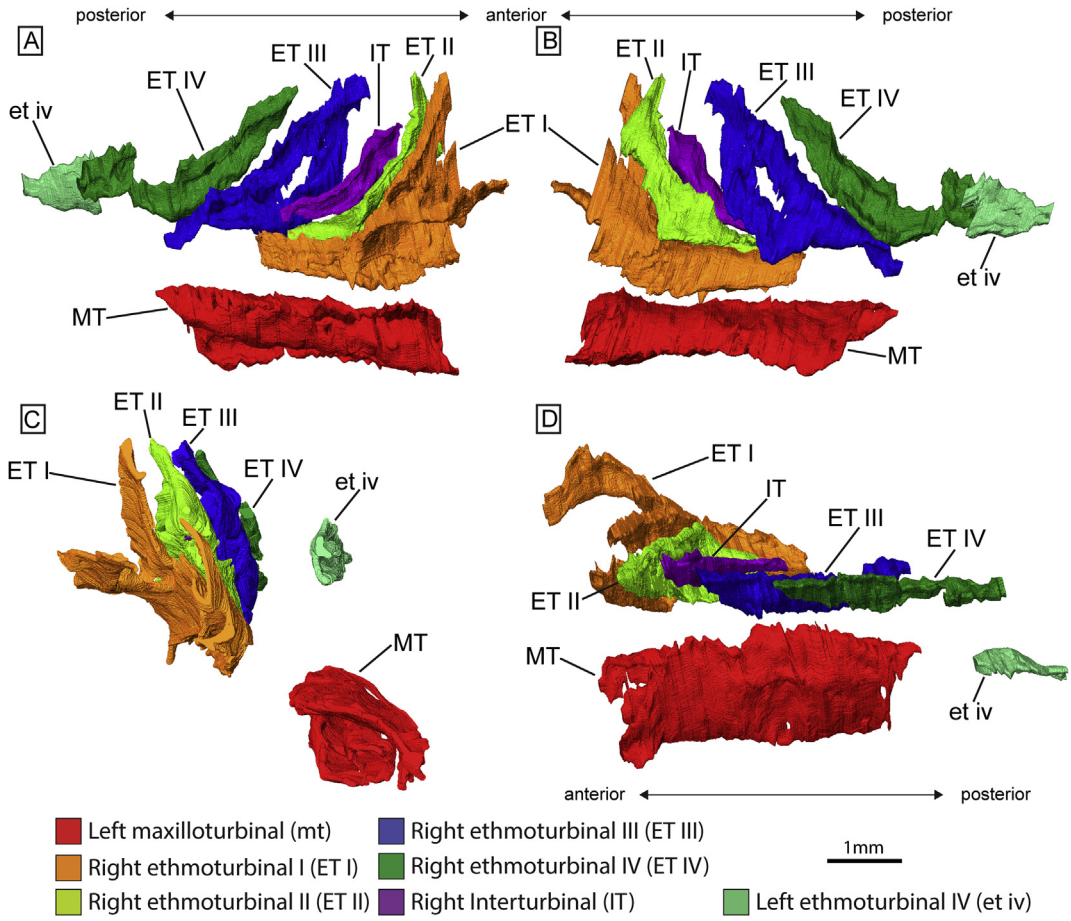

Figure 2. Three-dimensional rendering of digitally segmented turbinals in the right (ethmoturbinals I–IV, interturbinal) and left (maxilloturbinal, ethmoturbinal IV) nasal fossae of the *Shoshonius cooperi* specimen CM 31366: A) right lateral; B) left lateral; C) anterior; D) superior views. All turbinals shown in situ with the surrounding matrix and bone removed. Scale bar = 1 mm.

primates demonstrate some lability in this feature, the condition seen in *Shoshonius* and crown haplorhines is clearly derived compared with both strepsirrhines and nonprimate euarchontans (Rossie and Smith, 2007; Rossie et al., 2018; Lundeen and Kirk, 2019).

Taken as a whole, observations of cranial anatomy in *Shoshonius* made since the initial descriptions by Beard and colleagues (Beard et al., 1991; Beard and MacPhee, 1994) provide only limited new information regarding the phylogenetic affinities of the taxon. Although the lack of extreme reduction of the stapedial canal favors the hypothesis that *Shoshonius* is not a crown haplorhine, the presence of an AIOS and a vertical NLC are consistent with either stem haplorhine or stem tarsiiform status. We examined μCT scans of four *Shoshonius* crania that were made at higher resolution than those used for the preliminary report[1] of Rossie and Beard (2004). Although all four crania are damaged to varying degrees, these scans provide important new details regarding the internal cranial anatomy of *Shoshonius*. Here, we assess the anatomy of the nasal cavity and interorbital region of these specimens with the specific goal of determining whether *Shoshonius* exhibits derived features shared with either crown Haplorhini or crown Tarsiiformes.

2. Materials and methods

Crania CM 31367 and CM 60494 of *S. cooperi* were scanned at the University of Texas High-Resolution X-Ray Computed Tomography Scanning Facility (UTCT) in Austin, Texas, USA. Both scans were made using a North Star Imaging scanner with a Fein Focus High Power source at 130 kV and 0.14 mA. The resulting scans have 15.7 μm isometric voxels. Crania CM 31366 and CM 60493 were scanned at Duke University's Shared Materials Instrumentation Facility in Durham, North Carolina, USA. All scans of these specimens were made using a Nikon XTH 225 ST scanner. Initial scans at 145 kV and 0.067 mA yielded resolutions of 14.3 μm for CM 31366 and 12.8 μm for CM 60493. After the identification of turbinals in CM 31366, the rostrum of this specimen was rescanned at 120 kV and 0.074 mA to yield a scan with 8.9 μm isometric voxels. All scans of *Shoshonius* and additional scanning parameters are available for download from MorphoSource at https://www.morphosource.org/ (see Supplementary Online Material [SOM] Table S1). Extant taxa depicted here were downloaded from MorphoSource (SOM Table S1).

Data sets for each cranium were rendered as 3D volumes in Avizo version 8.1 (Visualization Sciences Group, Berlin). Images of turbinals in *Shoshonius* shown in Figures 1–4 are derived from the 8.9 μm resolution scan of CM 31366. Turbinals of this specimen were manually segmented in each slice using the brush tool. Bony nasal structures in extant taxa were segmented using the brush tool to select the approximate nasal cavity space occupied by the

[1] Based on μCT scans with ~30-μm resolution.

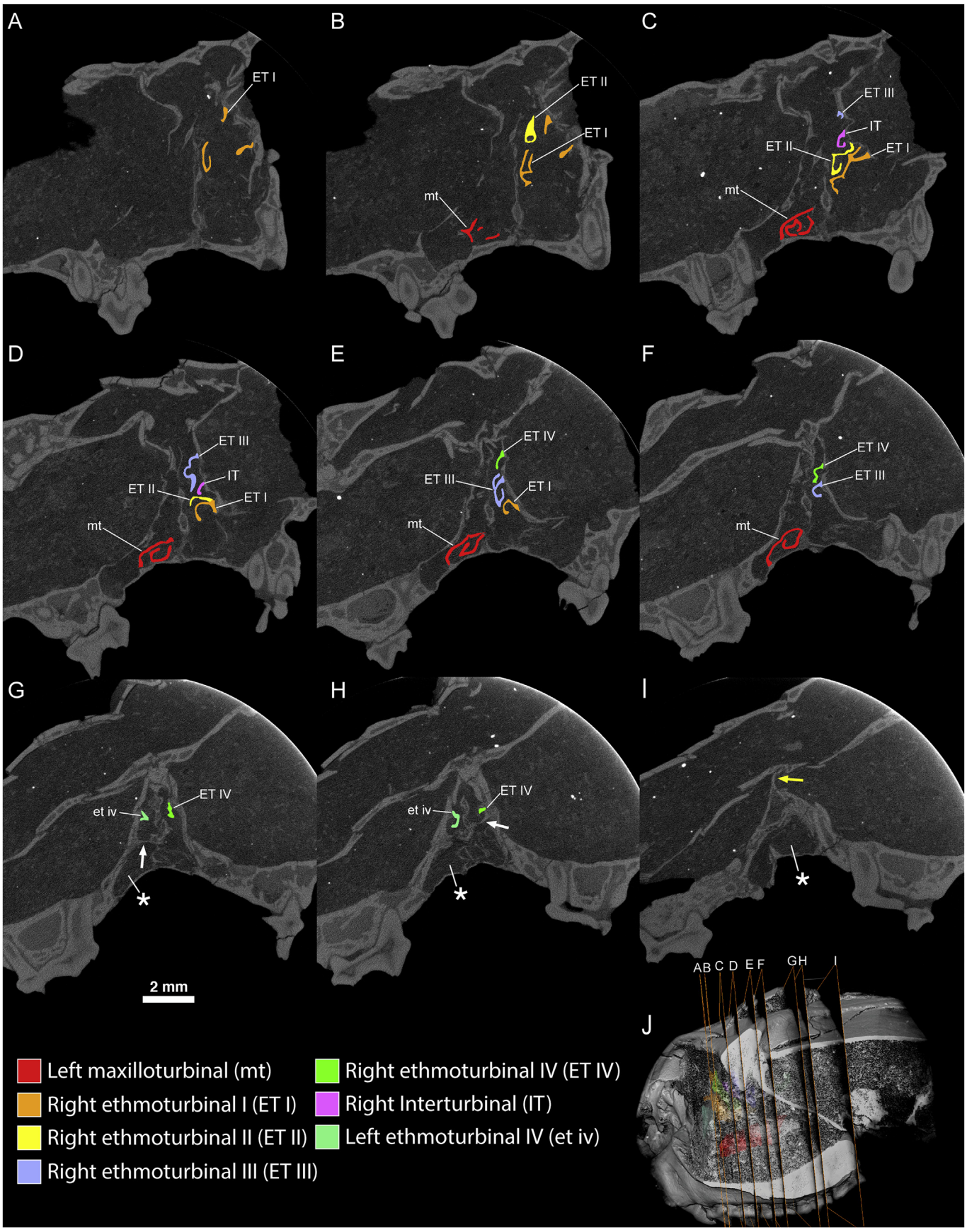
A
ET I
B
ET II
ET I
mt
C
ET III
IT
ET II
ET I
mt
D
ET III
IT
ET II
ET I
mt
E
ET IV
ET III
ET I
mt
F
ET IV
ET III
mt
G
ET IV
et iv
*
2 mm
H
ET IV
et iv
*
I
*
J
AB C D E F
GH
I
Left maxilloturbinal (mt)
Right ethmoturbinal I (ET I)
Right ethmoturbinal II (ET II)
Right ethmoturbinal III (ET III)
Right ethmoturbinal IV (ET IV)
Right Interturbinal (IT)
Left ethmoturbinal IV (et iv)

structure and then the thresholding tool to select only the grayscale values representing bone. Figures were created using Adobe Illustrator CS6 version 16.0.1 and Adobe Photoshop version 12.0.1 (Adobe Inc., San Jose). Terminology and criteria for demarcating structures of the nasal cavity follow Lundeen and Kirk (2019) and references therein (primarily Smith and Rossie, 2008).

3. Results and discussion

3.1. Specimen condition

The nasal cavities of CM 31367 (SOM Fig. S1) and CM 60493 are transversely compressed, and the turbinals are highly comminuted. As a result, some turbinal basal laminae are identifiable along the lateral walls of the nasal fossae in CM 31367 and CM 60493, but these specimens provide little useful information regarding turbinal morphology. The nasal cavity of CM 60494 (SOM Fig. S2) is obliquely crushed and distorted so that the upper surface of the nasal cavity exhibits a rightward lateral shift relative to the floor of the nasal cavity and palate. The posterior-most nasal cavity, including the olfactory recess, is badly damaged by crushing and several large cracks, and the interorbital septum and orbitosphenoid are partly destroyed by a zone of apparent chemical weathering that passes obliquely through the specimen. However, the nasal cavity of CM 60494 includes portions of the olfactory turbinals (sensu Lundeen and Kirk, 2019) and their primary laminae, the nasal septum, and the transverse lamina. Among the olfactory turbinals, ethmoturbinal I and the nasoturbinal are most readily identifiable. CM 60494 is also the only specimen with a cribriform plate that is largely intact.

Uniquely among the specimens analyzed here, crushing of CM 31366 occurred primarily in a dorsoventral direction. As a result, the braincase of CM 31366 is highly distorted and flattened, but the nasal and interorbital regions were spared the transverse crushing that obscures the anatomy of these regions in CM 60493 and CM 31367. Damage to the nasal cavity and interorbital region in CM 31366 primarily consists of dorsoventral foreshortening associated with collapse of the olfactory fossa, a right lateral shift of the roof of the nasal cavity, and buckling of the nasal septum, interorbital septum, and lateral walls of the nasal fossae. Nevertheless, the nasal cavity of CM 31366 exhibits the best turbinal preservation of the *Shoshonius* crania examined here (Figs. 1–4). The right nasal fossa contains large portions of ethmoturbinals I–IV and interturbinal I, including their basal laminae and contacts with the lateral wall. It should be noted, however, that none of these turbinals are preserved in their entirety, and the anterior portion of ethmoturbinal I is clearly missing. The olfactory turbinals are poorly preserved in the left nasal fossa, although a large segment of the posterior portion of ethmoturbinal IV is preserved in situ within the olfactory recess (Fig. 3G, H; SOM Fig. S3). Damage to the superior nasal cavity has also destroyed much of the nasoturbinals and cribriform plate. The maxilloturbinal is present bilaterally, but is best preserved in the left nasal fossa and is detached and translated medially in the right nasal fossa.

3.2. Turbinal number and morphology

The crania examined here provide unequivocal evidence that each nasal fossa of *Shoshonius* contained at least 4 ethmoturbinals, 1 maxilloturbinal, 1 nasoturbinal, and 1 interturbinal. In this respect, *Shoshonius* is primitive, as the last common ancestors of both Euarchonta and Primates probably possessed 4–5 ethmoturbinals, 1 maxilloturbinal, 1 nasoturbinal, 1 interturbinal, and 2 frontoturbinals (Lundeen and Kirk, 2019). Although the number and disposition of frontoturbinals is unknown in *Shoshonius* due to damage in the specimens examined here, it is clear that *Shoshonius* lacks the derived reduction in olfactory turbinal number shared by extant haplorhines (Figs. 1, 4; Smith and Rossie, 2006; Lundeen and Kirk, 2019). Living tarsiers and anthropoids are highly distinctive among mammals in retaining (at most) only 2 ethmoturbinals, 1 nasoturbinal, and 1 maxilloturbinal in each nasal fossa. Accordingly, all frontoturbinals, the interturbinal, and 2–3 ethmoturbinals are most parsimoniously interpreted as having been lost in the haplorhine stem linage (Lundeen and Kirk, 2019).

Furthermore, CM 31366 demonstrates that at least one turbinal (ethmoturbinal II) had a bullar anterior margin (Fig. 3B)—a primitive morphology that is shared with tarsiers but is lost in extant anthropoids (Lundeen and Kirk, 2019). Damage to the remaining ethmoturbinals makes it impossible to assess whether they also exhibited bullar anterior margins. CM 60494 also reveals that at least some of the olfactory turbinals of *Shoshonius* directly contacted the cribriform plate at their posterosuperior margins (SOM Fig. S2B). In this respect, *Shoshonius* is plesiomorphic and differs from extant haplorhines, which (with the exception of *Aotus*) lack direct contact between their olfactory turbinals and the cribriform plate (Lundeen and Kirk, 2019). Nevertheless, the olfactory turbinals of *Shoshonius* are distinctive in having primary laminae that are obliquely oriented, with the anterior end of the primary lamina substantially more dorsally positioned than the posterior end. A similar orientation of the olfactory turbinal primary laminae is seen in some extant haplorhines (e.g., *Procolobus badius* and *Hylobates lar*; Lundeen and Kirk, 2019). By comparison, most extant strepsirrhines have olfactory turbinal primary laminae that are obliquely oriented, but with the posterior end of the primary lamina substantially more dorsally positioned than the anterior end (Lundeen and Kirk, 2019).

3.3. Olfactory recess

The olfactory recess of *Shoshonius* is a blind cul-de-sac in the posterosuperior nasal cavity. In terms of its anatomy, position, and

Figure 3. Successive coronal cross sections through the nasal fossa of the *Shoshonius cooperi* specimen CM 31366 (indicated in J). Slices shown are as follows: A) 1249; B) 1222; C) 1137; D) 1065; E) 968; F) 904; G) 727; H) 678; I) 485. The full scan (https://doi.org/10.17602/M2/M56827) is available for download at https://www.morphosource.org/. White arrows in G, H = transverse lamina forming the floor of the olfactory recess; yellow arrow in I = apical interorbital septum. White asterisk in G–I = nasopharyngeal meatus. The better-preserved left maxilloturbinal is highlighted in red in B–F. Although the left maxilloturbinal is dorsoventrally compressed and has a damaged anterior margin (B), the scrolled cross section of this turbinal is clearly visible in C–F. Right ethmoturbinal (ET) I is highlighted in orange in A–E. The anterior end of right ET I is also clearly damaged (A, B), so it is not possible to determine if this turbinal had an enclosed, bullar (blister- or bubble-shaped) anterior margin as in nonanthropoid euarchontans (Lundeen and Kirk, 2019). As in most strepsirrhines (Lundeen and Kirk, 2019), ET I is positioned anterior and ventral to ETs II–IV (C–E). Right ET II is highlighted in yellow in B–D. A cross section through the bullar anterior margin of ET II is visible in B. At its posterior end (D), the primary lamina of right ET II merges with the primary lamina of ET I. The right interturbinal is highlighted in pink in C–D. The preserved portion of the right interturbinal is a simple scroll located dorsal to ET II and ventral to ET III. Like other interturbinals (Lundeen and Kirk, 2019), the preserved right interturbinal of *Shoshonius* does not extend as far medially into the nasal cavity as the ETs. Right ET III, which is located dorsal to ET II and ventral to ET IV, is highlighted in blue in C–F. At least part of right ET III has a double-scrolled cross section, with separate dorsal and ventral scrolls attached to the primary lamina (E). Right ET IV is highlighted in lighter green in E–H, and left ET IV is highlighted in darker green in G–H. At least the posterior portion of ET IV was bilaterally housed within the olfactory recess, as both turbinals are positioned dorsal to the transverse lamina (white arrows) in G–H. Scale bar = 2 mm. (For interpretation of the references to color in this figure legend, the reader is referred to the Web version of this article.)

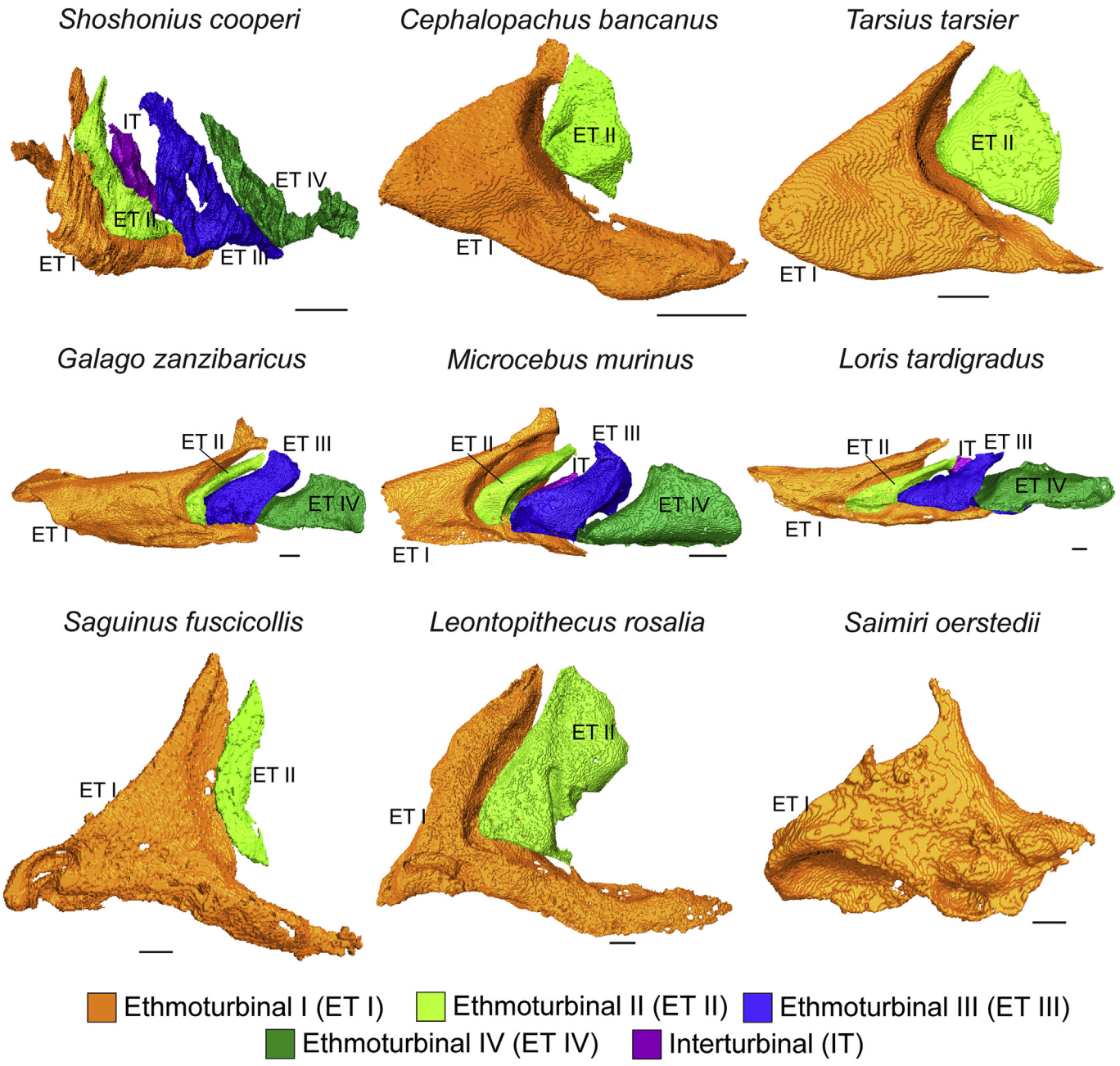

Figure 4. Medial view of olfactory turbinals in the right nasal fossa of selected small primates, including *Shoshonius* and tarsiers (top row), strepsirrhines (middle row), and anthropoids (bottom row). Scans of extant taxa were downloaded from MorphoSource (SOM Table S1). Specimens: *Shoshonius cooperi*, CM 31366; *Cephalopachus bancanus*, USNM 317189; *Tarsius tarsier*, USNM 200279; *Galago zanzibaricus*, MCZ 38912; *Microcebus murinus*, AMNH 185621; *Loris tardigradus*, BAA 0006; *Saguinus fuscicollis*, MCZ 15324; *Leontopithecus rosalia*, AMNH 235274; *Saimiri oerstedii*, MCZ 10131. Nasoturbinals and frontoturbinals are not shown because these structures are either poorly preserved or missing in CM 31366. Scale bars = 1 mm.

relationships with surrounding structures, the olfactory recess of *Shoshonius* is broadly similar in morphology to that of extant strepsirrhines, dermopterans, and scandentians (Lundeen and Kirk, 2019). It is located between the anterior cranial fossa superiorly and the nasopharyngeal meatus inferiorly. As in living nonhaplorhine euarchontans, the olfactory recess contains the posterior portion of ethmoturbinal IV and is separated from the nasopharyngeal meatus by a transverse bony lamina (Figs. 1 and 3; SOM Fig. S3; Lundeen and Kirk, 2019). Although the olfactory recess is visible in CM 31367 and CM 60494 (SOM Figs. S1 and S2), it is best preserved in CM 31366 (Figs. 1 and 3; SOM Fig. S3). In this latter specimen, the olfactory recess is about 2.1 mm in total anteroposterior length, or ~8.6% of the preserved cranial length (25.3 mm). However, this percentage is approximate because the anterior margin of the transverse lamina is incomplete, and total cranial length would be slightly greater in an undamaged specimen (~27.8–29.2 mm; Beard et al., 1991). *Shoshonius* is clearly plesiomorphic compared with extant haplorhines in retaining an olfactory recess. Indeed, an

olfactory recess housing ethmoturbinal IV (and often including portions of additional olfactory turbinals as well) occurs in all extant euarchontans except tarsiers and anthropoids, which lack an olfactory recess and ethmoturbinal IV (Smith and Rossie, 2006; Lundeen and Kirk, 2019).

3.4. Interorbital septum and olfactory fossa

All specimens of *Shoshonius* examined here exhibit an AIOS (sensu Cartmill, 1972 and Ross, 1994) between the medial apices of the left and right orbits (Fig. 3; SOM Fig. S1). As in many small-bodied extant haplorhines, the AIOS of *Shoshonius* consists of a single lamina of bone located posterior to the nasal cavity, anterior to the optic foramina, and inferior to the anterior cranial fossa. Contrary to the preliminary descriptions of this region based on lower resolution μCT scans (Rossie and Beard, 2004; Smith and Rossie, 2006), the greatest approximation between the orbits lies posterior to the olfactory recess (Fig. 1; SOM Fig. S1), and the AIOS does not replace the olfactory recess. *Shoshonius* thus differs from extant strepsirrhines and nonprimate euarchontans, which lack an AIOS (Ross, 1994). Although some small extant strepsirrhines exhibit a narrowing of the interorbital region immediately anterior to the optic foramina (e.g., *Galago zanzibaricus* in Fig. 1C; Simons and Rasmussen, 1989), such narrowings are bilaminar and differ fundamentally in both extent and morphology from the haplorhine AIOS (Ross, 1994; E.C.K., pers. obs.). These observations suggest that the AIOS of *Shoshonius* may be a derived feature shared with extant haplorhines. Nevertheless, the AIOS of *Shoshonius* is proportionally smaller than those of living tarsiers and small anthropoids. The total anteroposterior length of the AIOS is 1.2 mm in CM 60493 and 1.3 mm in CM 31366, or ~4.2–4.4% of cranial length. The AIOS is best preserved in CM 31367 (SOM Fig. S1), in which it measures 1.8 mm in estimated dorsoventral height and 1.9 mm in anteroposterior length (i.e., 6.5–6.8% of the cranial length). By comparison, the AIOS of USNM 317189 (Fig. 1; *Cephalopachus bancanus*) is typical for tarsiers. It consists of a bilaminar anterior portion 3.0 mm in anteroposterior length and a unilaminar posterior portion 5.3 mm in anteroposterior length. The unilaminar portion alone comprises 13.6% of total cranial length. Similarly, the AIOS of MCZ 15324 (Fig. 1D; *Saguinus fuscicollis*) is typical for callitrichines, measuring 7.8 mm in anteroposterior length or 13.6% of the total cranial length. Accordingly, as a percentage of cranial length, the AIOS of *Shoshonius* appears to be approximately half the size of that found in extant small haplorhines.

The olfactory fossa of *Shoshonius*, which in life accommodated the olfactory bulbs, was located dorsal to the olfactory recess and posterior olfactory turbinals (Fig. 1; SOM Figs. S1 and S2). In this respect, *Shoshonius* is similar to extant strepsirrhines and nonprimate euarchontans (Lundeen and Kirk, 2019). Although the olfactory fossa in *Shoshonius* may differ from these taxa in extending anterior to the olfactory recess, the degree of any such a forward projection of the olfactory fossa is obscured by damage to the specimens examined here. Nevertheless, it is clear that *Shoshonius* lacked the derived condition observed in living tarsiers, in which the olfactory fossa is displaced posteriorly and lies dorsal to the AIOS (Fig. 1B). As a result, the tarsier olfactory fossa is connected to the posterosuperior nasal cavity by a long and narrow 'tubus olfactorius' containing the olfactory nerves (Cartmill, 1972; Starck, 1984). The cribriform plate of tarsiers lies at the anterior terminus of the tubus olfactorius, dorsal to ethmoturbinal II (Fig. 1B; Lundeen and Kirk, 2019). By comparison, the cribriform plate of *Shoshonius* forms the anterior floor of the olfactory fossa, as in most other mammals (Fig. 1; SOM Fig. S2).

4. Conclusions

The nasal cavity and interorbital region of *Shoshonius* exhibit a number of key features that are probably plesiomorphic for primates, including the presence of 4 ethmoturbinals and 1 interturbinal in each nasal fossa, direct contact between the olfactory turbinals and cribriform plate, and the presence of an olfactory recess containing ethmoturbinal IV. These primitive features are noteworthy because extant haplorhines share the derived loss of all but 2 ethmoturbinals, loss of the interturbinal, loss of direct contact between the olfactory turbinals and the cribriform plate, and loss of the olfactory recess. *Shoshonius* further differs from living tarsiers in lacking the derived tubus olfactorius and posterior displacement of the olfactory fossa despite having very large orbits for its cranial size (Beard et al., 1991; Kay and Kirk, 2000). These attributes provide additional support for the hypothesis that *Shoshonius* is not a crown haplorhine (Ross, 1994; Kay et al., 2008). Indeed, extant tarsiers and anthropoids share a constellation of derived features of the nasal fossa, orbit (postorbital septum), middle ear (anterior accessory cavity and transverse septum), and cranial circulation ('perbullar' internal carotid path, extreme reduction or loss of the stapedial canal) that are demonstrably absent in *Shoshonius*. Nevertheless, *Shoshonius* resembles small extant haplorhines in possessing a unilaminar AIOS. This derived feature is absent in at least one Eocene primate—*Rooneyia viejaensis*—that has traditionally been classified as an omomyoid (Ross, 1994; Kirk et al., 2014; Lundeen and Kirk, 2019). Combined with the observation that *Shoshonius* (but not *Rooneyia*) also possesses a vertical NLC (Rossie et al., 2018), the AIOS of *Shoshonius* adds further weight to the argument that Omomyoidea is paraphyletic (Beard et al., 1991; Beard and MacPhee, 1994; Ross, 1994; Kay et al., 2008). These observations favor a reinterpretation of the various cranial character states shared by *Shoshonius* and extant tarsiers (Beard and MacPhee, 1994). If *Shoshonius* is a stem haplorhine that is more closely related to crown haplorhines than other omomyoids, then features such as 'peaked' choanae and basioccipital and basisphenoid bullar flanges may initially have evolved in the haplorhine stem lineage and subsequently been lost in the anthropoid stem lineage. Alternatively, these features may have evolved independently in *Shoshonius* and extant tarsiers. Regardless of these questions regarding the sequence of character evolution, the preponderance of newly available evidence based on μCT data presented here and in other studies (Boyer et al., 2016; Rossie et al., 2018) provides robust support for the conclusion that *Shoshonius* is a stem haplorhine and not a stem tarsiiform.

Acknowledgments

This analysis would not have been possible without the generous assistance of Doug Boyer, who scanned CM 31366 and CM 60493 at the Duke University Shared Materials Instrumentation Facility and subsequently made these scans available for the research described in this article. Matt Colbert, Jessie Maisano, and the staff of UTCT provided expert assistance with μCT scanning at UT Austin. John Wible and Amy Henrici provided access to specimens at the Carnegie Museum of Natural History and assistance with loans. Pauline Coster and Chris Beard provided assistance with specimen transport. Chris Beard, Doug Boyer, Rich Kay, Callum Ross, James Rossie, Erik Seiffert, and Blythe Williams provided useful discussions of cranial anatomy in *Shoshonius*. Kari Allen, Doug Boyer, Lynn Copes, Justin Gladman, Lauren Gonzales, Randi Griffin, and Lynn Lucas made their scans of extant primates available through MorphoSource. James Rossie generously shared scans of CM 60493 and CM

31366 made at UTCT in 2002, a copy of the PowerPoint file from his 2004 Society of Vertebrate Paleontology talk, and an unpublished draft of a manuscript on the internal cranial anatomy of *Shoshonius*. Tim Ryan kindly allowed us to examine a μCT scan of CM 60494 made at the Center for Quantitative Imaging at Pennsylvania State University. David Alba, James Rossie, Mary Silcox, and an anonymous reviewer provided excellent suggestions for the revision of this manuscript.

Supplementary Online Material

Supplementary online material to this article can be found online at https://doi.org/10.1016/j.jhevol.2020.102748.

References

Beard, K.C., MacPhee, R.D.E., 1994. Cranial anatomy of *Shoshonius* and the antiquity of the Anthropoidea. In: Fleagle, J.G., Kay, R.F. (Eds.), Anthropoid Origins. Plenum Press, New York, pp. 55–97.

Beard, K.C., Krishtalka, L., Stucky, R.K., 1991. First skulls of the early Eocene primate *Shoshonius cooperi* and the anthropoid-tarsier dichotomy. Nature 349, 64–67.

Boyer, D.M., Seiffert, E.R., Gladman, J.T., Bloch, J.I., 2013. Evolution and allometry of calcaneal elongation in living and extinct primates. PLoS One 8 e67792.

Boyer, D.M., Kirk, E.C., Silcox, M.T., Gunnell, G.F., Gilbert, C.C., Yapuncich, G.S., Allen, K.L., Welch, E., Bloch, J.I., Gonzales, L.A., Kay, R.F., Seiffert, E.R., 2016. Internal carotid arterial canal size and scaling in Euarchonta: Re-assessing implications for arterial patency and phylogenetic relationships in early fossil primates. J. Hum. Evol. 97, 123–144.

Cartmill, M., 1972. Arboreal adaptations and the origin of the order Primates. In: Tuttle, R. (Ed.), The Functional and Evolutionary Biology of Primates. Aldine-Atherton, Chicago, pp. 97–122.

Cartmill, M., 1980. Morphology, function and evolution of the anthropoid postorbital septum. In: Ciochon, R., Chiarelli, A.B. (Eds.), Evolutionary Biology of New World Monkeys and Continental Drift. Plenum Press, New York, pp. 243–274.

Cartmill, M., Kay, R.F., 1978. Craniodental morphology, tarsier affinities, and primate suborders. In: Chivers, D.J., Joysey, K.A. (Eds.), Recent Advances in Primatology, vol. 3. Academic Press, London, pp. 205–214.

Dagosto, M., Gebo, D.L., Beard, K.C., 1999. Revision of the Wind River faunas, early Eocene of central Wyoming. Part 14. Postcranium of *Shoshonius cooperi* (Mammalia: Primates). Ann. Carnegie Mus. 68, 175–211.

Granger, W., 1910. Tertiary faunal horizons in the Wind River Basin, Wyoming, with descriptions of new Eocene mammals. Bull. Am. Mus. Nat. Hist. 28, 235–251.

Heesy, C.P., Ross, C.F., 2001. Evolution of activity patterns and chromatic vision in primates: morphometrics, genetics and cladistics. J. Hum. Evol. 40, 111–149.

Kay, R.F., Kirk, E.C., 2000. Osteological evidence for the evolution of activity pattern and visual acuity in primates. Am. J. Phys. Anthropol. 113, 235–262.

Kay, R.F., Simons, E.L., Ross, J.L., 2008. The basicranial anatomy of African Eocene/Oligocene anthropoids. Are there any clues for platyrrhine origins? In: Fleagle, J.G., Gilbert, C.C. (Eds.), Elwyn Simons: A Search For Origins. Springer, New York, pp. 125–158.

Kirk, E.C., Daghighi, P., Macrini, T.E., Bhullar, B.A.S., Rowe, T.B., 2014. Cranial anatomy of the Duchesnean primate *Rooneyia viejaensis*: new insights from high resolution computed tomography. J. Hum. Evol. 74, 82–95.

Lundeen, I.K., Kirk, E.C., 2019. Internal nasal morphology of *Rooneyia viejaensis* and extant Euarchonta: using μCT scan data to understand and infer patterns of nasal fossa evolution in primates. J. Hum. Evol. 132, 137–173.

MacPhee, R.D.E., Cartmill, M., 1986. Basicranial structures and primate systematics. In: Swindler, D., Erwin, T. (Eds.), Comparative Primate Biology, Systematics, Evolution, and Anatomy, vol. 1. Alan R. Liss, New York, pp. 219–275.

Muchlinski, M.N., Kirk, E.C., 2017. A comparative analysis of infraorbital foramen size in Paleogene euarchontans. J. Hum. Evol. 105, 57–68.

Ni, X., Gebo, D.L., Dagosto, M., Meng, J., Tafforeau, P., Flynn, J.J., Beard, K.C., 2013. The oldest known primate skeleton and early haplorhine evolution. Nature 498, 60–64.

Ni, X., Li, Q., Li, L., Beard, K.C., 2016. Oligocene primates from China reveal divergence between African and Asian primate evolution. Science 352, 673–677.

Ross, C.F., 1994. The craniofacial evidence for anthropoid and tarsier relationships. In: Fleagle, J.G., Kay, R.F. (Eds.), Anthropoid Origins. Plenum Press, New York, pp. 469–547.

Ross, C.F., Williams, B.A., Kay, R.F., 1998. Phylogenetic analysis of anthropoid relationships. J. Hum. Evol. 35, 221–306.

Rossie, J.B., Beard, K.C., 2004. Intracranial anatomy of *Shoshonius cooperi* (Tarsiiformes, primates) as revealed by high-resolution computed tomography. J. Vertebr. Paleontol. 24, 106A.

Rossie, J.B., Smith, T.D., 2007. Ontogeny of the nasolacrimal duct in primates: functional and phylogenetic implications. J. Anat. 210, 195–208.

Rossie, J.B., Smith, T.D., Beard, K.C., Godinot, M., Rowe, T.B., 2018. Nasolacrimal anatomy and haplorhine origins. J. Hum. Evol. 114, 176–183.

Seiffert, E.R., Simons, E.L., Boyer, D.M., Perry, J.M., Ryan, T.M., Sallam, H.M., 2010. A fossil primate of uncertain affinities from the earliest late Eocene of Egypt. Proc. Natl. Acad. Sci. U.S.A. 107, 9712–9717.

Seiffert, E.R., Boyer, D.M., Fleagle, J.G., Gunnell, G.F., Heesy, C.P., Perry, J.M.G., Sallam, H.M., 2018. New adapiform primate fossils from the late Eocene of Egypt. Hist. Biol. 30, 204–226.

Silcox, M.T., Bloch, J.I., Boyer, D.M., Godinot, M., Ryan, T.M., Spoor, F., Walker, A., 2009. Semicircular canal system in early primates. J. Hum. Evol. 56, 315–327.

Simons, E.L., Rasmussen, D.T., 1989. Cranial morphology of *Aegyptopithecus* and *Tarsius* and the question of the tarsier-anthropoidean clade. Am. J. Phys. Anthropol. 79, 1–23.

Smith, T.D., Rossie, J.B., 2006. Primate olfaction: anatomy and evolution. In: Brewer, W.J., Castle, D., Pantelis, C. (Eds.), Olfaction and the Brain. Cambridge University Press, Cambridge, pp. 135–166.

Smith, T.D., Rossie, J.B., 2008. Nasal fossa of mouse and dwarf lemurs (Primates, Cheirogaleidae). Anat. Rec. 291, 895–915.

Starck, D., 1984. The nasal cavity and nasal skeleton of *Tarsius*. In: Niemitz, C. (Ed.), Biology of Tarsiers. Gustav Fischer Verlag, Stuttgart, pp. 275–290.

Szalay, F.S., 1976. Systematics of the Omomyidae (Tarsiiformes, Primates): taxonomy, phylogeny, and adaptations. Bull. Am. Mus. Nat. Hist. 156, 157–450.

Szalay, F.S., Delson, E., 1979. Evolutionary History of the Primates. Academic Press, San Diego.